J Fluoresc (2014) 24:1849–1859
DOI 10.1007/s10895-014-1473-1

ORIGINAL PAPER

Mapping the ATP Binding Site in the Plasma Membrane H^+-ATPase from *Kluyveromyces lactis*

José G. Sampedro · Hugo Nájera · Salvador Uribe-Carvajal · Yadira G. Ruiz-Granados

Received: 1 July 2014 / Accepted: 13 October 2014 / Published online: 28 October 2014
© Springer Science+Business Media New York 2014

Abstract The plasma membrane H^+-ATPase from *Kluyveromyces lactis* contains 14 tryptophan residues. Binding a nucleotide or unfolding with Gnd-HCl quenched intrinsic fluorescence by≈60 % suggesting that in the H^+-ATPase-Nucleotide complex there is solvent-mediated collisional quenching of W505 fluorescence. *N*-bromosuccinimide (NBS) treatment of H^+-ATPase modified a single W residue in both native and Gnd-HCl-unfolded H^+-ATPase. Denaturing the H^+-ATPase with 1 % SDS led to expose six tryptophan residues while requiring 17 NBS/H^+-ATPase. The remaining eight tryptophan residues kept buried indicating a highly stable TM domain. Acrylamide generated static quenching of fluorescence; partial in the native enzyme (V= 0.43 M^{-1}) and complete in the Gnd-HCl-unfolded H^+-ATPase (V= 0.81 M^{-1}). Collisional quenching (K_{sv}) increased from 3.12 to 7.45 M^{-1} upon H^+-ATPase unfolding. W505 fluorescence titration with NBS yielded a molar ratio of 6 NBS/H^+-ATPase and quenched≈60 % fluorescence. In the recombinant N-domain, the distance between W505 and MantATP was estimated to be 21 Å by FRET. The amino acid residues involved in nucleotide binding were identified by N-domain molecular modelling and docking with ATP. In the N-domain/ATP complex model, the distance between W505 and ATP was 20.5 Å. ATP binding leads to a conformational change in the N-domain of H^+-ATPase that exposes W505 to the environment.

Keywords H^+-ATPase · Chemical modification · Tryptophan fluorescence · UV spectroscopy · FRET

J. G. Sampedro (✉)
Departamento de Biofísica, Instituto de Física, Universidad Autónoma de San Luis Potosí, Manuel Nava 6, Zona Universitaria, C.P. 78290 San Luis Potosí, SLP, México
e-mail: jg.sampedro@gmail.com

H. Nájera
Departamento de Ciencias Naturales, Universidad Autónoma Metropolitana Cuajimalpa (UAM-C), Pedro Antonio de los Santos 84, San Miguel Chapultepec C.P. 11850, D.F, México

S. Uribe-Carvajal · Y. G. Ruiz-Granados
Departamento de Genética Molecular, Instituto de Fisiología Celular (IFC-UNAM), Ciudad de México C.P. 04510, D.F, México

Introduction

The plasma membrane H^+-ATPase (Pma1; E.C. 3.6.1.35) from the yeast *Kluyveromyces lactis* is a P-ATPase [1]. The H^+-ATPase pumps protons from the cell using the free energy of ATP hydrolysis to generate a pH gradient, which is used for secondary transport of nutrients and inorganic ions across the plasma membrane [2].

The H^+-ATPase structure contains (based on 3D modelling) a transmembrane (TM) domain and four cytoplasmic domains that display specific motions during the catalytic cycle [3]. These are the: a) N-domain; which binds ATP, b) P-domain; that becomes transitorily phosphorylated at an Asp residue, c) A-domain; which transmits the motion from the cytoplasmic domains to the TM α-helices resulting in H^+ transport, and d) R-domain; which upon activation by glucose becomes phosphorylated [3]. The binding of P-ATPases to ATP and ion(s) has been studied by intrinsic protein fluorescence [4]. Fluorescence variations have been generally small (1–4 %) in Ca^{2+}-ATPase and other P-ATPases. However, large intrinsic fluorescence quenching (≈ 60 %) has been observed in the H^+-ATPase from *K. lactis* [5]. Fluorescence quenching was useful to calculate the affinity of the N-domain for ADP and ATP [5]. Solvent exposure of the tryptophan residue located at the N-domain was proposed to be the cause of fluorescence quenching [5]. However, the H^+-ATPase from *K. lactis* does contain numerous tryptophan residues (most of

them at the TM domain) that might contribute to variations in fluorescence (Fig. 1).

In this work the H^+-ATPase from *K. lactis* was purified and both fluorescence and UV-absorbance spectra were obtained and analysed in order to establish a) the contribution of tryptophan residues to intrinsic fluorescence, b) the chemical reactivity of the different tryptophan residues to *N*-bromosuccinimide (NBS) under native and different denatured states, and c) the exposure extent of the N-domain tryptophan under native and denatured states. The distance between W505 and ATP was determined by FRET using MantATP (a fluorescent ATP analogue) and a heterogously expressed N-domain of the H^+-ATPase. The results were confirmed by molecular docking using a three-dimensional model of the N-domain. Putative amino acid residues involved in ATP binding were identified.

Experimental

Materials and Methods

Guanidine hydrochloride (Gnd-HCl), Adenosine 5′-(β,γ-imido)triphosphate (AMP-PNP), *N*-tetradecyl-*N*,*N*-dimethyl-3-ammonium-1-propanesulfonate (Zwittergent 3,15), trehalose and *N*-bromosuccinimide (NBS), were from Sigma

```
seq  MSAATEPTKE KPVNNQDSDD EDEDIDQLIE DLQSHHGLDD ESEDDEHVAA    50
pred IIIIIIIIII IIIIIIIIII IIIIIIIIII IIIIIIIIII IIIIIIIIII

seq  GSARPVPEEL LQTDPSYGLT SDEVTKRRKK YGLNQMSEET ENLFVKFLMF   100
pred IIIIIIIIII IIIIIIIIII IIIIIIIiii iiiiiiiiii iiHHHHHHHH

seq  FIGPIQFVME AAAILAAGLE DWVDFGVICG LLFLNAAVGF IQEYQAGSIV   150
pred HHHHHHHHHH HHHHHHHooo ooooohhhhh hhhhhhhhhh hhhhhhhhhh
       TM1                                  TM2
seq  DELKKTLANS AVVIRDGNLV EVPSNEVVPG DILQLEDGVV IPADGRLVTE   200
pred iiiiiiiiii iiiiiIIIII IIIIIIIIII IIIIIIIIII IIIIIIIIII

seq  DCFIQIDQSA ITGESLAVDK RFGDSTFSSS TVKRGEAFMI VTATGDSTFV   250
pred IIIIIIIIII IIIIIIIIII IIIIIIIIII IIIIIIIIII IIIIIIIIII

seq  GRAAALVNKA AAGSGHFTEV LNGIGTILLI LVIVTLLLVW VASFYRTNKI   300
pred IIIIiiiiii iiiiiiiiiH hhhhhhhhhh hhhhhhhhhh hhhhoooooo
                                      TM3
seq  VRILRYTLAI TIVGVPVGLP AVVTTTMAVG AAYLAKKQAI VQKLSAIESL   350
pred ooooooooHH HHHHHHHHHH HHHHHHHHHH HHHiiiiiii iiiiiiiiII
                            TM4
seq  AGVEILCSDK TGTLTKNKLS LHEPYTVEGV DPDDLMLTAC LAASRKKKGL   400
pred IIIIIIIIII IIIIIIIIII IIIIIIIIII IIIIIIIIII IIIIIIIIII

seq  DAIDKAFLKS LISYPRAKAA LTKYKLLEFH PFDPVSKKVT AIVESPEGER   450
pred IIIIIIIIII IIIIIIIIII IIIIIIIIII IIIIIIIIII IIIIIIIIII
                            N-domain
Seq  IICVKGAPLF VLKTVEEEHP IPEDVRENYE NKVAELASRG FRALGVARKR   500
pred IIIIIIIIII IIIIIIIIII IIIIIIIIII IIIIIIIIII IIIIIIIIII

seq  GEGHWEILGV MPCMDPPRDD TAQTVNEARH LGLRVKMLTG DAVGIAKETC   550
pred IIIIIIIIII IIIIIIIIII IIIIIIIIII IIIIIIIIII IIIIIIIIII

seq  RQLGLGTNIY NAERLGLGGG GDMPGSELAD FVENADGFAE VFPQHKYNVV   600
pred IIIIIIIIII IIIIIIIIII IIIIIIIIII IIIIIIIIII IIIIIIIIII

seq  EILQQRGYLV AMTGDGVNDA PSLKKADTGI AVEGATDAAR SAADIVFLAP   650
pred IIIIIIIIII IIIIIIIIII IIIIIIIIII IIIIIIIIII IIIIIIIIII

seq  GLSAIIDALK TSRQIFHRMY SYVVYRIALS LHLEIFLGLW IAILNRSLNI   700
pred IIIiiiiiii iiiiiiiiHH HHHHHHHHHH HHHHHHHHHH HHHooooooo
                                      TM5
seq  DLVVFIAIFA DVATLAIAYD NAPYSPKPVK WNLRRLWGMS VILGIILAIG   750
pred ohhhhhhhhh hhhhhhhhhi iiiiiiiiii iiiiihhhhh hhhhhhhhhh
       TM6                                                TM7
seq  TWITLTTMFV PKGGIIQNFG SIDGVLFLQI SLTENWLIFI TRAAGPFWSS   800
pred HHHHHHHHHH ooooooooHH HHHHHHHHHH HHHHHHHHHH Hiiiiiiiii
                                      TM8
seq  IPSWQLSGAV LIVDIIATMF CLFGWWSQNW NDIVTVVRVW IFSFGVFCVM   850
pred iiiiiiiHHH HHHHHHHHHH HHHHHooooo oooHHHHHHH HHHHHHHHHH
                     TM9                    TM10
seq  GGAYYMMSES EAFDRFMNGK SRRDKPSGRS VEDFLMAMQR VSTQHEKEN    899
pred HHHHHHHHii iiiiiiiiii iiiIIIIIII IIIIIIIIII IIIIIIIII
```

Fig. 1 Transmembrane α-helix prediction for the plasma membrane H^+-ATPase from *K. lactis*. The amino acid sequence of the plasma membrane H^+-ATPase was submitted to http://www.enzim.hu/hmmtop/index.php for transmembrane (TM) α-helices prediction. Amino acid residues predicted to be part of TM α-helices: TM1 93–117,TM2 126–150, TM3 270–294, TM4 309–333, TM5 669–693, TM6 702–719, TM7 736–760, TM8 769–791, TM9 808–825, and TM10 834–858. Predicted amino acid states are: inside loop (*I*), membrane helix (*H*), inside TM α-helix tail (*i*), and outside TM α-helix tail (*o*). Tryptophan (*W*) residues are highlighted. Amino acid sequence comprising the N-domain is *underlined*

Chemical Co. (St. Louis, MO). Acrylamide was from Bio Rad. Zymolyase-20T was from ICN Pharmaceuticals Inc. (Costa Mesa, CA). All other reagents were of the best quality available commercially.

Purification of the Plasma Membrane H^+-ATPase

The plasma membrane was isolated from *K. lactis* by differential centrifugation. Then the H^+-ATPase was purified by ultracentrifugation in a discontinuous trehalose concentration gradient as described by Sampedro et al. [5, 6]. The pellets were suspended in a small volume of 1 mM EGTA-Tris, pH 6.8 and kept at −70 °C until used. On SDS-PAGE, the 100,000 M_r band corresponding to the plasma membrane H^+-ATPase was ≥95 % by densitometry. The H^+-ATPase specific activity was 18.6±0.3 μmol Pi mg prot^{-1} min^{-1} at 25 °C. H^+-ATPase concentration was determined spectrophotometrically at 280 nm using a molar extinction coefficient of 107,300 M^{-1} cm^{-1}.

Synthesis of the H^+-ATPase N-domain Gene, Protein Expression and Purification

The cDNA coding for the plasma membrane H^+-ATPase N-domain was synthesized *de novo* by GeneScript Corporation (Piscatway, NJ, USA) and cloned in-frame into the *EcoRI* and *NotI* sites of vector pGS-21a. *E. coli* BL-21(DE3) cells were transformed with plasmid pGS-21a, containing the DNA insert. Expression and purification of the recombinant N-domain was performed as described by Pihlajamaa et al. [9] with some modifications [5].

Synthesis of N-methylanthraniloyl-ATP

The fluorescent molecule 2′(3′)-*O*-*N*-Methylanthraniloyl ATP (MantATP) was synthesized as described by Hiratsuka [10], purified by column chromatography and stored at −72 °C until use. MantATP was tested for purity by thin-layer chromatography on silica gel plates. MantATP concentration was determined using a molar extinction coefficient of 23,300 M^{-1} cm^{-1} at 255 nm.

H^+-ATPase Intrinsic Fluorescence Quenching Induced by Nucleotide Binding or by Gnd-HCl

H^+-ATPase intrinsic fluorescence spectra were recorded in a Shimadzu RF 5301 spectrofluorophotometer equipped with a thermostated cell chamber and constant stirring as described by Sampedro et al. [5]. Briefly, H^+-ATPase (0.1 μM) was suspended in 20 mM phosphate buffer, pH 6.8, 5 mM $MgCl_2$. Then after 1 min (to allow equilibration), the steady state fluorescence emission spectra were recorded at 300–450 nm using an excitation wavelength of 290 nm; at this wavelength the ATP inner filter effect is minimal. Then, AMP-PNP (5 mM) was added from a 0.5 M stock solution and fluorescence spectra were obtained and corrected for dilution and inner filter effect. For the H^+-ATPase unfolding assay, 6 M Gnd-HCl was included in the incubation buffer and fluorescence spectra were obtained. Experiments were performed three times and standard deviation (SD) was less than 5 %.

H^+-ATPase UV Absorbance Spectra and Tryptophan Titration with NBS

The UV absorbance spectrum was obtained for the native H^+-ATPase (11 μM) suspended in 2 mL of 20 mM phosphate buffer, pH 7.0. NBS reactive tryptophan residues (solvent exposed) were titrated in the H^+-ATPase by stepwise addition of 5 μL NBS (10 mM stock solution). After each NBS addition the UV absorbance spectrum was obtained. Tryptophan reactivity to NBS was also tested under two different unfolded states: a) in partially unfolded H^+-ATPase incubated in 6 M GndHCl, which promotes unfolding of the cytoplasmic hydrophilic domains P, A, and N only, and b) fully unfolded H^+-ATPase incubated in 1 % SDS; which unfolds the whole H^+-ATPase including the highly hydrophobic α-helices at the TM domain. After equilibration, NBS aliquots (5 μL) were added stepwise and the UV absorbance spectra were recorded after each addition. Experiments were performed three times and SD was less than 5 %. Data analysis was performed as described below.

H^+-ATPase Tryptophan Fluorescence Titration with NBS

Tryptophan titration was performed as described by Peterman and Laidler [7]. Briefly, the H^+-ATPase (0.1 μM) was suspended in 20 mM phosphate buffer pH 6.8 and intrinsic fluorescence was titrated by stepwise addition of aliquots (5 μl) of a 2 mM NBS aqueous stock solution. After 3 min, the H^+-ATPase fluorescence emission spectrum (300–450 nm) was recorded exciting at 290 nm. Fluorescence intensity at 325 nm was used for data analysis. Experiments were performed three times and SD was less than 5 %. Data analysis was performed as described below.

H^+-ATPase Fluorescence Quenching by Acrylamide

The fluorescence of native and denatured (6 M Gnd-HCl) H^+-ATPase (suspended in 20 mM phosphate buffer pH 6.8) was quenched by the stepwise addition of small aliquots (25 μl) of an 8 M acrylamide solution. After each addition, the fluorescence emission spectrum (300–450 nm) was obtained exciting at 290 nm [8]. Fluorescence intensity at 325 nm was used to analyse the tryptophan exposure degree in both, native and denatured H^+-ATPase. Experiments were performed three

times and in all cases SD was less than 5 %. Data analysis was performed as described below.

Fluorescence Resonance Energy Transfer

FRET experiments were performed using an isolated, purified recombinant H^+-ATPase N-domain and the fluorescent ATP analogue MantATP. H^+-ATPase N-domain (0.1 μM final concentration) was suspended in 20 mM phosphate buffer, pH 6.8 and 5 mM $MgCl_2$. After addition (2 μl) of MantATP from a 0.5 M stock solution the suspension was allowed to equilibrate 1 min and then the fluorescence spectra were recorded at 300–550 nm using an excitation wavelength of 275 nm and a 5 nm slit. The steady state fluorescence of MantATP at 405 nm was used for data analysis. Experiments were performed three times and SD was less than 5 %.

Data Analysis

The NBS-mediated chemical modification of H^+-ATPase tryptophan residues is a result of the oxidation of indole to oxindole; a weak absorbing chromophore. Indole oxidation results in a decrease of absorbance intensity at 280 nm [11]. The number of tryptophan residues modified by NBS per H^+-ATPase molecule (native or unfolded) was calculated using Eq. 1 as described by Spande and Witktop [11].

$$Tryptophans/H^+\text{-}ATPase = \frac{\Delta Abs_{280nm} \times 1.31}{5,500 \times H^+\text{-}ATPase} \quad (1)$$

where ΔAbs_{280nm} is the change in H^+-ATPase absorbance intensity after each NBS addition, 5,500 is the tryptophan molar absorption coefficient. The maximum number of NBS reactive tryptophans was determined when no further change in absorbance was observed.

H^+-ATPase fluorescence quenching by acrylamide was analysed using the Stern-Volmer equation (Eq. 2) as described by Eftink and Ghiron [8].

$$F_0/F = (1 + K_{sv} \cdot Q) \cdot e^{V \cdot Q} \quad (2)$$

where F_0 and F are the fluorescence intensities at 325 nm in the absence and presence of the quencher (Q); respectively. The static (V) and collisional (K_{sv}) quenching constants were calculated by non-linear regression using the iterative software Microcal Origin 6.0© (Northampton, MA).

FRET efficiency (E) was calculated as the fractional decrease of donor fluorescence (F_0) in the presence of acceptor (F) MantATP as described in Eq. 3 [12].

$$E = 1 - \left(\frac{F}{F_0}\right) \quad (3)$$

E is also related to the distance (R) between fluorescence donor and acceptor as described in Eq. 4.

$$E = \frac{1}{1 + \left(\frac{R}{R_0}\right)^6} \quad (4)$$

where R_0 is the Föster distance; a sigmoid dependence of E versus R is observed [13]. Föster distance (in Å) is given by equation 5 (Eq. 5) [13, 14].

$$R_0 = 0.211\left[\kappa^2 \cdot n^{-4} \cdot Q_D \cdot J(\lambda)\right]^{\frac{1}{6}} \quad (5)$$

where κ^2 is the orientation factor assumed usually as 2/3, n is the refractive index with value close to that of water (n=1.33), Q_D is the quantum yield of donor (Q_D for tryptophan is 0.12) [15] and $J(\lambda)$ is the overlap integral which express the degree of spectral overlap between tryptophan fluorescence emission and anthroyl acceptor absorbance [13]. R_0 for tryptophan (as energy donor) and anthroyl group (as energy acceptor) has been determined and is 25 Å [12]. Thus, the distance (R) between W505 and MantATP was calculated using Eq. 6.

$$R = \left(\frac{1}{E} - 1\right)^{\frac{1}{6}} \cdot R_0 \quad (6)$$

Results and Discussion

The N-domain of the H^+ATPase from *K. lactis* Contains a Single Tryptophan

The plasma membrane H^+-ATPase from *K. lactis* was purified as described before [5]. Protein purity was >95 % as evaluated by densitometry (Results not shown). H^+-ATPase kinetics were sigmoid and parameters were essentially similar to those reported before [5]. The H^+-ATPase from *K. lactis* contains 14 tryptophan residues (Fig. 1) [1]. The H^+-ATPase crystal structure is still unavailable; however a three dimensional model (PDB code 1MHS) has been generated for H^+-ATPase from *Neurospora crassa*. In this study, the three dimensional model for H^+-ATPase from *K. lactis* was generated using the IntFOLD

server. Analysis of the H^+-ATPase structural model showed a sole tryptophan residue located at the cytoplasmic portion of the enzyme (at the N-domain) while the remaining tryptophan residues were at the transmembrane α-helices (Fig. 2a) [3].

The H^+-ATPase N-domain is Predicted to Undergo a Conformational Change Upon ATP Binding that Exposes W505 to the Solvent

It has been reported that binding of either ATP or ADP quenches (≈ 60 %) the H^+-ATPase intrinsic fluorescence [5]. Based on NMR data from Na^+,K^+-ATPase ligand binding, we propose a structural dynamic model which describes the molecular mechanism responsible for intrinsic fluorescence quenching (Fig. 2b) [5]. In the model, the N-domain tryptophan 505 (W505) becomes exposed to the aqueous solvent as a result of the ATP binding-induced movement of the 5β sheet-loop-6β sheet motif [5, 16]. N-domain structural dynamics seem to be independent from the whole protein, nonetheless hinging on the P-domain [16]. Due to this independence, ATP binding would not affect the tryptophan residues at the TM domain, and thus these would not contribute to fluorescence quenching (Fig. 2b).

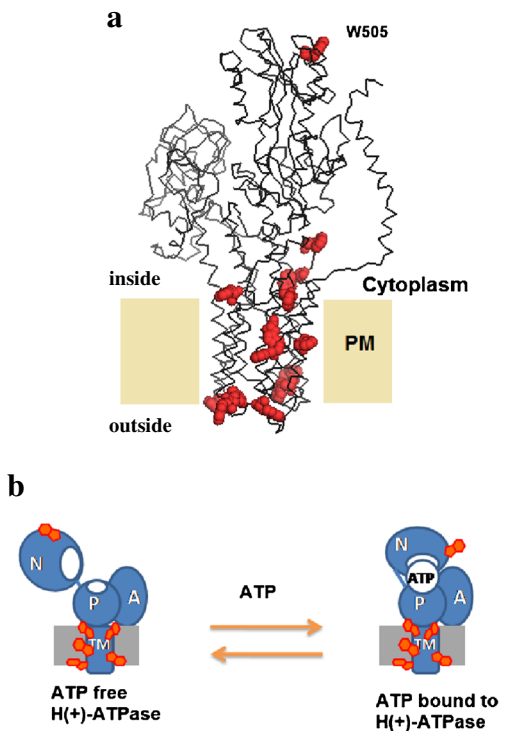

Fig. 2 Location of tryptophan residues in the plasma membrane H^+-ATPase. **a** Three dimensional model of the H^+-ATPase from *Kluyveromyces lactis*. H^+-ATPase contains 14 tryptophan residues, W505 is located at the nucleotide-binding domain (N-domain) in the large cytoplasmic portion of the enzyme. The other 13 tryptophan residues are positioned at α-helices in the transmembrane domain (TM). **b** Cartoon illustrating the N-domain movement performed after ATP binding. W505 exposes to solvent when ATP binds at the active site

Different Treatments of the H^+-ATPase Expose a Tryptophan to the Aqueous Solvent

In the presence of 6 M Gnd-HCl, partial chemical denaturation of the H^+-ATPase resulted in exposure of a tryptophan, probably W505 (Fig. 3a), leading to≈63.5 % decrease in fluorescence; which was essentially similar to the quenching mediated by the ATP analogue AMP-PNP at 5 mM (Fig. 3b). The Gnd-HCl-mediated unfolding affects solely the cytoplasmic portion of the H^+-ATPase leaving the TM segments unaffected [17]. The results above suggest that exposure of W505 is the cause of fluorescence quenching in the plasma membrane H^+-ATPase.

The H^+-ATPase UV absorbance spectra were analysed in order to test the exposure of W505 in the native enzyme both in the Gnd-HCl-denatured H^+-ATPase and in the SDS-denatured H^+-ATPase (Fig. 4a). Each of the two denatured H^+-ATPases exhibited decreased absorbance as compared to the native enzyme (Fig. 4a). Similar UV-Vis absorbance spectra were observed for both (Gnd-HCl and SDS) denatured enzymes (Fig. 4a).

NBS reacts with solvent exposed tryptophan residues [11]. The NBS reaction with tryptophan residues forms oxindole, thus decreasing absorbance at 280 nm while increasing absorbance at 250 nm [11]. In the native H^+-ATPase the stepwise addition of NBS decreased absorbance at 280 nm (Δ_{abs}= 0.025–0.035 AU) while it promoted an increase at 250 nm (Fig. 4b). In the Gnd-HCl-denatured H^+-ATPase the decrease at 280 nm was similar to the pattern observed for the native H^+-ATPase, while at 250 nm absorbance increased many times more (Fig. 4c). In the SDS-denatured H^+-ATPase the absorbance intensity decrease at 280 nm was many times larger than to the other conditions and in addition, the increase in absorbance at 250 nm was even larger than in the Gnd-HCl-treated H^+-ATPase (Fig. 4d). The similar decrease in the 280 nm absorbance intensity for native and Gnd-HCl-denatured H^+-ATPase suggested that both states have the same number of exposed tryptophan residues. While in the SDS denatured H^+-ATPase the increase in quenching suggests that a large number of tryptophan residues were reactive to NBS. Thus the SDS treatment likely unfolded the TM domain of the H^+-ATPase.

Both in the Native and in a Partially Denatured H^+-ATPase a Single Tryptophan is Exposed, While Further Denaturing Exposes More Tryptophan Residues

The maximum number of tryptophan(s) modified by NBS in a given H^+-ATPase state was determined using the absorbance intensity change at 280 nm (ΔAbs_{280nm}) (Fig. 5) and Eq. 1 [11]. In addition, the NBS molecules per H^+-ATPase required to modify all reachable tryptophan residue(s) was determined (Fig. 5) [11]. In the native H^+-ATPase, ΔAbs_{280nm} analysis

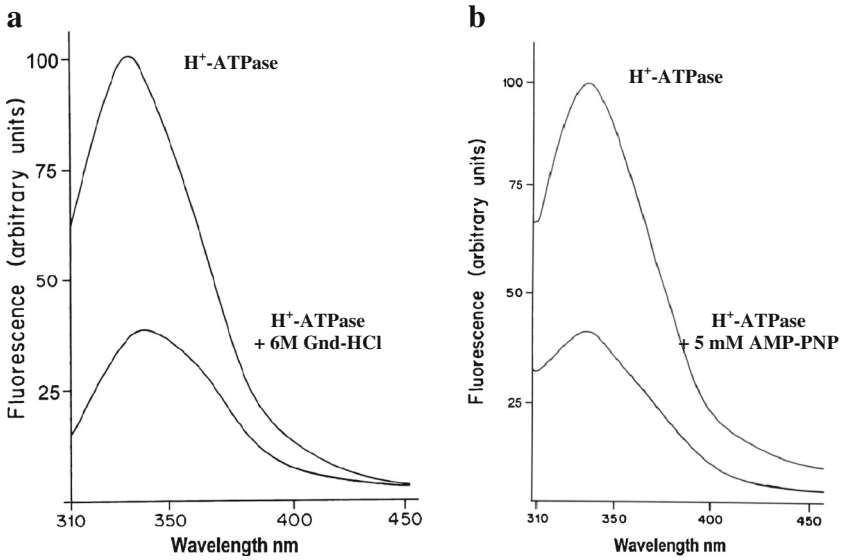

Fig. 3 Quenching of the plasma membrane H^+-ATPase intrinsic fluorescence. **a** Unfolded H^+-ATPase. The purified native H^+-ATPase (0.1 μM) was suspended in 20 mM phosphate buffer, pH 6.8, 5 mM $MgCl_2$ and after 1 min incubation, the steady state fluorescence spectrum was obtained by exciting at 290 nm. H^+-ATPase was unfolded by the presence of 6 M Gnd-HCl. **b** ATP bound to H^+-ATPase. The non-hydrolysable ATP analogue AMP-PNP (5 mM) was included and steady state fluorescence emission spectra obtained. Fluorescence spectra were corrected for dilution and inner filter effect. Spectra are representative of three experiments

showed that a sole tryptophan residue was modified by NBS, requiring 5–6 NBS/H^+-ATPase (Fig. 5a). Similarly, in the Gnd-HCl denatured H^+-ATPase, ΔAbs_{280nm} analysis showed that just one tryptophan residue was modified by NBS. However, it required at least 15 NBS/H^+-ATPase (Fig. 5b), probably because of side reactions of NBS with other exposed aminoacid residues such as methionine, cysteine, hystidine, lysine or arginine [11]. Therefore, both in the native and Gnd-HCl-denatured H^+-ATPase, it is likely that NBS reacted with the same tryptophan residue, most likely the one at the N-

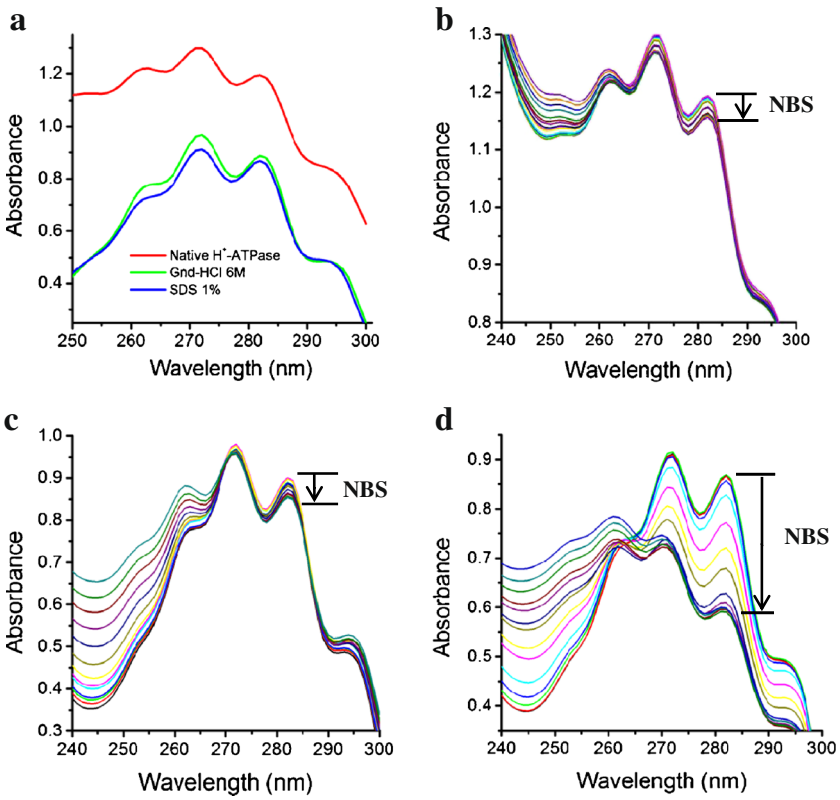

Fig. 4 UV-Vis absorbance spectra of the plasma membrane H^+-ATPase. **a** The H^+-ATPase (11 μM) was suspended in 2 mL of 20 mM phosphate buffer, pH 7.0 and where indicated 6 M Gnd-HCl or 1 % SDS was included. The UV-Vis absorbance spectra were obtained for native (*red line*), Gnd-HCl unfolded (*green line*) and SDS unfolded H^+-ATPase (*blue line*). **b** Native H^+-ATPase tryptophan titration. NBS (5 μL) was added stepwise from a 10 mM stock solution, after NBS addition and equilibration, the UV-Vis absorbance spectra were obtained. **c** Gnd-HCl unfolded H^+-ATPase. **d** SDS unfolded H^+-ATPase. In **c** and **d**, tryptophan titration with NBS was performed as described in **b**

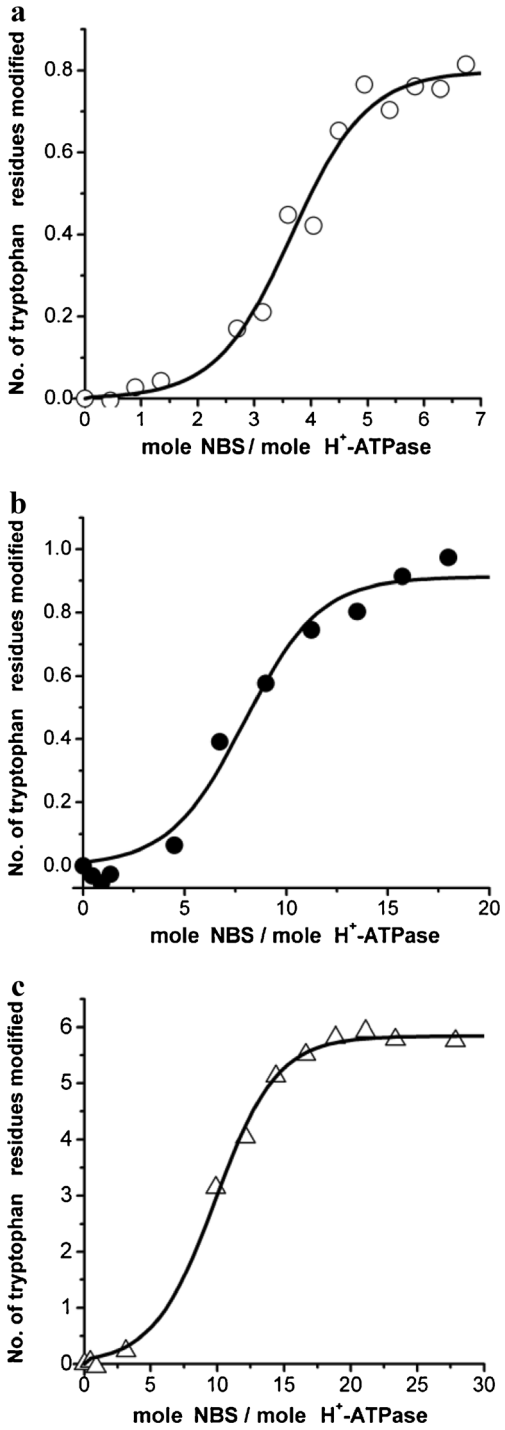

Fig. 5 Number of tryptophan residues modified versus NBS/H^+-ATPase molar ratio. The number of NBS modified tryptophan(s) was determined using Eq. 1 and ΔAbs_{280nm} from Fig. 4. The maximum number of modified tryptophan(s) was determined when ΔAbs_{280nm} reach zero, **a** native H^+-ATPase, **b** Gnd-HCl unfolded H^+-ATPase, and **c** SDS unfolded H^+-ATPase

domain (W505). In contrast, in the SDS-denatured H^+-ATPase, ΔAbs_{280nm} analysis showed that NBS modified 6 tryptophan residues requiring at least 20 NBS molecules/H^+-ATPase (Fig. 5c). Thus, SDS did partially unfold the TM domain exposing 5 TM tryptophan residues, probably W122, W731, W798, W804, and W830, which are located at the inside and outside tails of TM α-helices (Fig. 1). Interestingly, these tryptophan residues are located at the peptide segments connecting the TM α-helices, near the surface of the membrane (Fig. 1). The remaining (eight) tryptophan residues: W290, W690, W737, W752, W796, W825, W826, and W840 are probably fully embedded in the TM domain (Figs. 1 and 2a). Therefore, some tryptophan residues at the TM domain are not exposed even in the presence of a strong denaturing agent such as SDS (Figs. 4d and 5c). The results indicate that the cytoplasmic segments of the *K. lactis* plasma membrane H^+-ATPase are quite labile, while in contrast the TM domain seems to be highly stable; a property already deduced from freeze-drying and rehydration data [18].

The NBS-mediated chemical modification of the tryptophan residues in H^+-ATPase was further studied by fluorescence quenching. The number of NBS molecules required to modify the putative tryptophan at the N-domain was determined. Fluorescence quenching by NBS provides information about tryptophan location in the protein three-dimensional structure [7]. Tryptophan residues at the protein surface (solvent accessible) are more susceptible to be modified by NBS than those at the protein core or hydrophobic domains; i.e. those embedded in the TM domain [7]. H^+-ATPase fluorescence titration with NBS was biphasic. A straight linear fluorescence decrease (up to≈60 %) was observed at low NBS/H^+-ATPase molar ratios (Fig. 6a), which was followed by a second less pronounced fluorescence decrease at higher NBS/H^+-ATPase molar ratios (Fig. 6b). Therefore, in the native H^+-ATPase there seem to be two tryptophan populations displaying different reactivity to NBS; the first one is exposed and highly reactive while the second one is buried and less reactive. Interestingly, from the *x*-axis intercept it was calculated that 6 molecules of NBS/H^+-ATPase were necessary to quench 60 % of the H^+-ATPase fluorescence (Fig. 6b). The above was in agreement with the UV absorbance quenching analysis and suggests that W505 was modified at low NBS/H^+-ATPase molar ratios (Figs. 4b and 5a), while buried tryptophan residues at the TM domain required higher NBS/H^+-ATPase molar ratios (Figs. 5c and 6b). In agreement with our results, it has been reported that there are two tryptophan populations in the Ca^{2+}-ATPase that display different reactivity to fluorescence quenchers [19]. Also, the thirteen tryptophan residues at the TM-domain do not contribute significantly to total fluorescence, perhaps due to the short distances between them resulting in local energy transfer.

W505 is Near the Surface of the H^+-ATPase Structure

Acrylamide-mediated fluorescence quenching was used to further explore the solvent exposure extent of W505 in the native and the Gnd-HCl-denatured H^+-ATPase (Fig. 7). Fluorescence quenching data were analysed using the Stern-Volmer equation

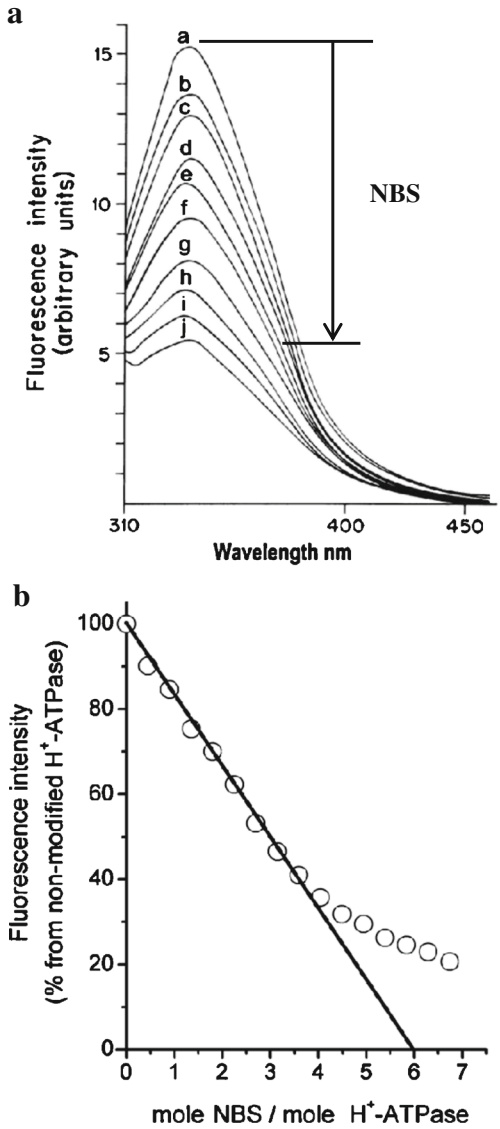

Fig. 6 NBS titration of the plasma membrane H^+-ATPase intrinsic fluorescence. **a** The H^+-ATPase (0.1 μM) was suspended in 20 mM phosphate buffer pH 6.8. Then NBS (5 μl) was added stepwise (a–j) from a 2 mM NBS aqueous stock solution. After 3 min incubation, the H^+-ATPase fluorescence emission spectra was recorded by exciting at 290 nm. **b** Plot of fluorescence intensity emission at 325 nm versus NBS/H^+-ATPase molar ratio. The steady state fluorescence emission at 325 nm was used for data analysis. The maximum number of tryptophan modified per H^+-ATPase was determined by linear regression at the *x*-axis interception of the straight line formed

(Eq. 2); where the static quenching parameter (V) provides information about tryptophan exposure. Acrylamide addition to both native and Gnd-HCl H^+-ATPase resulted in large fluorescence quenching (Fig. 7a and b). For the native H^+-ATPase, fluorescence intensity decreased 25 and 45 % in the presence of 0.1 and 0.2 M acrylamide respectively (Fig. 7a). In the Gnd-HCl-denatured H^+-ATPase, acrylamide induced fluorescence quenching (Fig. 7b). Interestingly, the Stern-Volmer plot displayed an upward line deviation indicating the existence of static quenching in both the native –H^+-ATPase and the Gnd-HCl-denatured H^+-ATPase (Fig. 7c). Static quenching occurs when tryptophan residues come into permanent physical contact with the acrylamide molecule [8, 20]. The static quenching (V) value represents the tryptophan exposure degree to the aqueous medium [8, 20]. For a fully exposed tryptophan residue V is 1 M^{-1} [8, 20]. While for the collisional quenching constant (K_{sv}), the value is 8 M^{-1}. For the native H^+-ATPase, fluorescence-quenching data were well fitted by non-linear regression to Eq. 2 (Fig. 7c). The calculated native H^+-ATPase quenching parameters were V=0.43±0.03 M^{-1} and K_{sv} =3.12± 0.11 M^{-1}. The above values indicated that W505 is partially exposed to the medium. In contrast, for the Gnd-HCl-denatured H^+-ATPase (Fig. 7b and c) K_{sv} =7.45±0.08 M^{-1} and V=0.81± 0.02 M^{-1}. Thus indicating as expected, that W505 was almost totally exposed [8, 20].

In a Recombinant, Isolated N-domain, the Distance Between W505 and the Nucleotide Binding Site is 21 Å

In order to eliminate all possible interference from other tryptophan residues, the N-domain was expressed in *E. coli* and purified to homogeneity [5]. The synthetic N-domain was used to measure the distance to a bound fluorescent ATP derivative by FRET. The isolated N-domain is known to display hyperbolic fluorescence quenching upon binding of ATP or ADP, indicating that the N-domain retains the ability to bind nucleotides [5]. The recombinant Cu^+-ATPase N-domain exhibits a similar behaviour [27]. W505 may behave as an energy donor for MantATP as suggested by observing that the N-domain fluorescence emission spectrum overlaps the excitation spectrum of MantATP (Fig. 8a). FRET spectra were obtained at different nucleotide concentrations, where the intensity of MantATP fluorescence (at 427 nm) increased with MantATP binding while the W505 fluorescence decreased (Fig. 8b). The observed hyperbolic pattern for energy transfer was dependent on MantATP concentration (Fig. 8c). The efficiency for energy transfer (E) was determined to be≈80 % (Fig. 8c), which led to calculate a distance between W505 and MantATP of 21 Å. Ion and nucleotide binding have been studied in some P-ATPases by intrinsic fluorescence variations, i.e. in the presence of Mg^{2+} the sarcoplasmic reticulum Ca^{2+}-ATPase fluorescence intensity increases (4 %) and undergoes a 2 nm blue shift [4], while in the presence of either ADP or ATP a slight fluorescence quenching of 4–6 and 0.5–1.0 % is observed, respectively [21, 22]. Small fluorescence quenching has also been observed in other P-type ATPases, i.e. Na^+,K^+-ATPase undergoes a 1–3 % fluorescence decrease in response to nucleotide binding [23]. Therefore, fluorescent nucleotides (TNP-ATP or Tb-FTP) or active site covalent-labels have been used to compensate the lack of significant intrinsic fluorescence variations [24, 25]. FRET has aided in the study of the oligomeric state of the Ca^{2+}-ATPase [26].

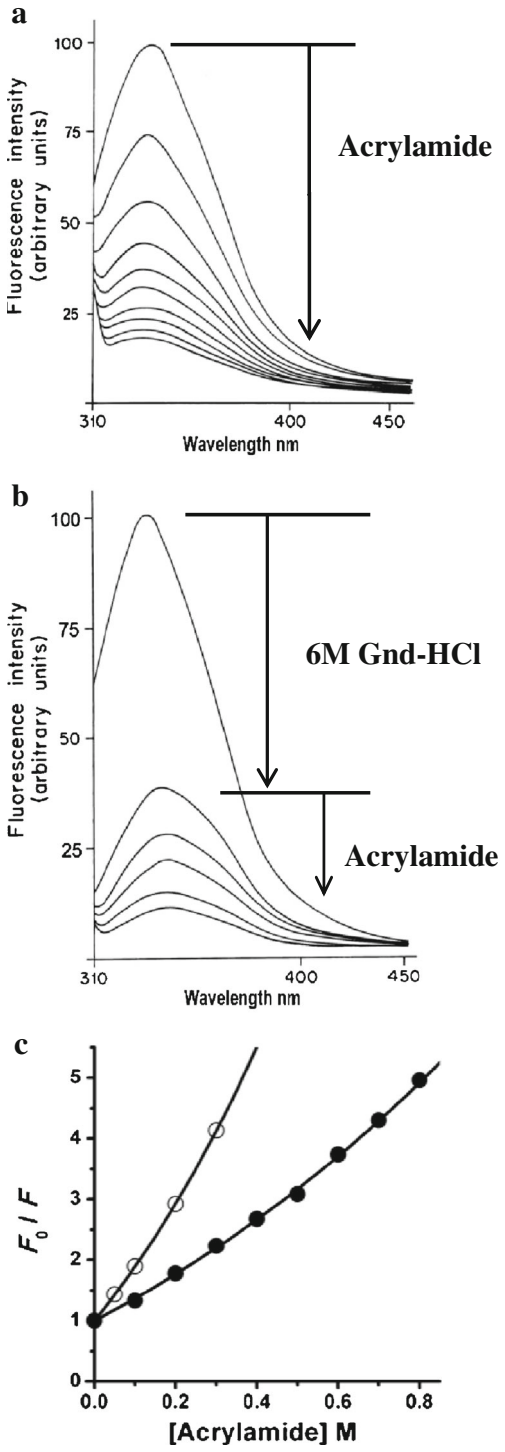

◀ **Fig. 7** Acrylamide-mediated quenching of the H^+-ATPase fluorescence. **a** Native H^+-ATPase. The H^+-ATPase was suspended in 20 mM phosphate buffer pH 6.8 and intrinsic fluorescence emission was quenched by stepwise addition of aliquots (25 μl) from an 8 M acrylamide solution. Then, fluorescence emission spectra were recorded upon excitation at 290 nm. **b** Unfolded H^+-ATPase. The H^+-ATPase was unfolded by the presence of 6 M Gnd-HCl. The residual H^+-ATPase fluorescence was quenched by acrylamide addition as described in **a. c** Stern-Volmer plot of data in A and B. Steady state fluorescence emission at 325 nm was used in Eq. 2 to determine static (V) and collisional quenching (K_{sv}) constants by non-linear regression. Quenching constants were: K_{sv} =3.12±0.11 M^{-1} and V=0.43±0.03 M^{-1} for native H^+-ATPase, and K_{sv} =7.45±0.08 M^{-1} and V=0.81±0.02 M^{-1} for Gnd-HCl denatured H^+-ATPase

N-domain Modelling and ATP Docking Identifies Putative ATP-binding Amino Acids

The N-domain overall folding structure is highly conserved in all P-type ATPases [28]. However, the amino acid sequence of the N-domain of the *K. lactis* H^+-ATPase is smaller than other P-type ATPases [16, 28], i.e. 40 % smaller than the Ca^{2+}-ATPase. To explore this, a three-dimensional model for the N-domain H^+-ATPase from *K. lactis* was generated using the IntFOLD server (http://www.reading.ac.uk/bioinf/IntFOLD/IntFOLD2_form.html). Then, the best model was selected based on a P-value cut off ($p<0.001$) and threaded to identify the ATP binding site using the COFACTOR server (http://zhanglab.ccmb.med.umich.edu/COFACTOR/). Results indicated that the following amino acid residues are involved in ATP binding: F432, V439, K455, G456, A457, R492, A493, and L494 (Fig. 9a). In Ca^{2+}-ATPase and in Na^+,K^+-ATPase, these same residues have been found to be important for nucleotide binding [29]. In the *K. lactis* H^+-ATPase N-domain, the model indicates that F432 and R492 residues interact directly with ATP (Fig. 9a). ΔG for ATP binding was −5 kJ/mol, as calculated with the Hyde software (BioSolveIT GmbH. Sank Augustin Germany).

In the N-domain:ATP complex model, a distance of≈ 20.5 Å was calculated between W505 and the 3OH group in the ribose moiety of ATP (Fig. 9a). The above was in good agreement to the experimental distance obtained by FRET (Results above). From these data it may be concluded that upon ATP binding the N-domain moves 5–7 Å in order to position the ATP γ-phosphate close to the aspartate residue at the P-domain and allow the phosphate transfer reaction. The role of the aminoacid residues in the P-domain is still to be determined [26]. The small size of the N-domain from *K. lactis* suggests that it may not contain more than the minimal structural requirements for both ATP binding and phosphate transfer and thus it is adequate to model ATP binding by P-ATPases.

The model also indicated that in the N-domain:ATP complex the indole group of W505 is exposed on the surface (Fig. 9b). This is in agreement with the quenching of fluorescence observed upon ligand binding [5], as well as with NBS-titration and acrylamide quenching results reported here. In contrast to W505 in the *K. lactis* H^+-ATPase, the corresponding W552 in the Ca^{2+}-ATPase N-domain (PDB 1SU4) is located in the protein core (in alpha helix 5), where the overall folding does not change

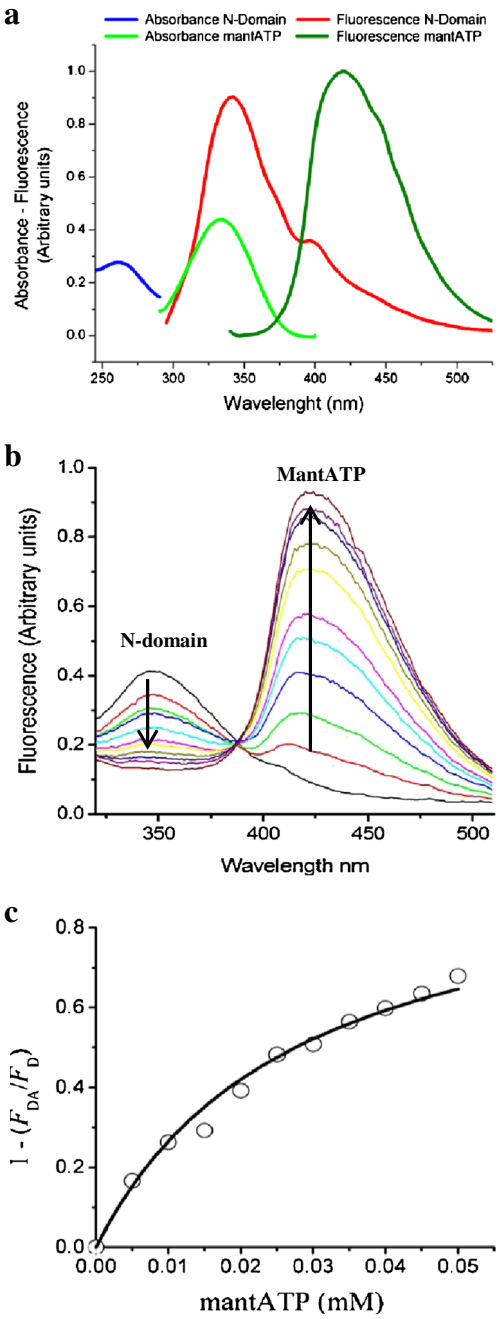

Fig. 8 Molecular distance measurement in N-domain H^+-ATPase by FRET. **a** Excitation and emission spectra for N-domain and MantATP. **b** FRET between N-domain and MantATP. **c** MantATP fluorescence intensity emission at 427 nm. The distance between W505 and the methylanthraniloyl group was 21 Å, and calculated using Eq. 4

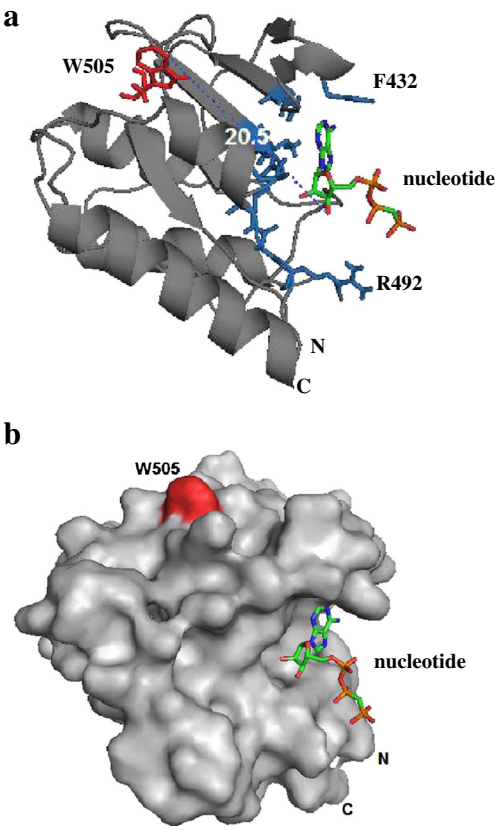

Fig. 9 H^+-ATPase N-domain three-dimensional model. **a** N-domain structural model. The 3D-model was generated using the IntFOLD server (http://www.reading.ac.uk/bioinf/IntFOLD/IntFOLD2_form.html). Nucleotide threading was obtained with COFACTOR server (http://zhanglab.ccmb.med.umich.edu/COFACTOR/). Amino acid residues (in *blue*) involved in nucleotide binding are F432, V439, K455, G456, A457, R492, A493, and L494. The amino acid residues involved in close interaction with the adenine nucleotide are F432 and R492. The distance between W505 and the adenine nucleotide was calculated to be 20.5 Å. **b** N-domain structural surface. W505 is exposed when adenine nucleotide is in complex with N-domain

upon AMP-PNP binding [30]. The absence of changes in W552 exposure is probably the reason for the absence of changes in the intrinsic fluorescence in Ca^{2+}-ATPase upon nucleotide binding [31].

In P-type ATPases, the N-domain has an essential role in the E1-to-E2 transition observed during the catalytic cycle and it interacts dynamically with P- and A-domains [28]. P-type ATPase mutations may cause human diseases, e.g. heart failure and Darier, Wilson and Menkes diseases [32, 33]. Some of these mutations are located at the N-domain and result in low ATPase activity, low affinity for substrates, ion transport deficiency and misfolding [32, 33]. As showed in this report, fluorescence is useful for studies of ligand binding, protein and domain stability, molecular distance determination, and catalytic step studies in membrane proteins. When present, intrinsic fluorescence may be useful to study protein oligomeric states in resting and active state, as well as the oligomerization pathway itself. In the H^+-ATPase of *K. lactis,* which exhibits high intrinsic fluorescence the effect of mutating important or essential amino acids on ATP binding and N-domain folding and stability may also be studied, shedding light on the pathophysiology of P-ATPases [34].

Acknowledgments This work was supported by grants from PROMEP-SEP UASLP-PTC-301 (PROMEP/103.5/10/4412) and SEP-CONACYT 156497.

References

1. Miranda M, Ramirez J, Pena A, Coria R (1995) Molecular cloning of the plasma membrane H(+)-ATPase from *Kluyveromyces lactis*: a single nucleotide substitution in the gene confers ethidium bromide resistance and deficiency in K^+ uptake. J Bacteriol 177:2360–2367
2. Serrano R, Kielland-Brandt MC, Fink GR (1986) Yeast plasma membrane ATPase is essential for growth and has homology with (Na^+/K^+), K^+- and Ca^{2+}-ATPases. Nature 319:689–693
3. Kühlbrandt W, Zeelen J, Dietrich J (2002) Structure, mechanism, and regulation of the *Neurospora* plasma membrane H^+-ATPase. Science 297:1692–1696
4. Dupont Y, Guillain F, Lacapere JJ (1988) Fluorimetric detection and significance of conformational changes in Ca^{2+}-ATPase. Methods Enzymol 157:206–219
5. Sampedro JG, Ruiz-Granados YG, Nájera H, Téllez-Valencia A, Uribe S (2007) Fluorescence quenching by nucleotides of the plasma membrane H^+-ATPase from *Kluyveromyces lactis*. Biochemistry 46: 5616–5622
6. Sampedro JG, Muñoz-Clares RA, Uribe S (2002) Trehalose-mediated inhibition of the plasma membrane H^+-ATPase from *Kluyveromyces lactis*: dependence on viscosity and temperature. J Bacteriol 184:4384–4391
7. Peterman BF, Laidler KJ (1980) Study of reactivity of tryptophan residues in serum albumins and lysozyme by *N*-bromosuccinamide fluorescence quenching. Arch Biochem Biophys 199:158–164
8. Eftink MR, Ghiron CA (1976) Exposure of tryptophanyl residues in proteins. Quantitative determination by fluorescence quenching studies. Biochemistry 15:672–680
9. Pihlajamaa T, Lankinen H, Ylostalo J et al (2004) Characterization of recombinant amino-terminal NC4 domain of human collagen IX. J Biol Chem 279:24265–24273
10. Hiratsuka T (1983) New ribose-modified fluorescent analogs of adenine and guanine nucleotides available as substrates for various enzymes. Biochim Biophys Acta 742:496–508
11. Spande TF, Witkop B (1967) Determination of the tryptophan content of proteins with N-bromosuccinimide. Methods Enzymol 11:498–506
12. Wu P, Brand L (1994) Resonance energy transfer: methods and applications. Anal Biochem 218:1–13
13. Lakowicz JR (2006) Principles of fluorescence spectroscopy. Kluwer, USA
14. Yengo CM, Chrin LR, Rovner AS, Berger CL (2000) Tryptophan 512 is sensitive to conformational changes in the rigid relay loop of smooth muscle myosin during the MgATPase. J Biol Chem 275: 25481–25487
15. Chen RF (1972) Measurements of absolute values in biochemical fluorescence spectroscopy. J Res Natl Bur Stand 76A(6):593–606
16. Hilge M, Siegal G, Vuister GW, Guntert P, Gloor SM, Abrahams JP (2003) ATP-induced conformational changes of the nucleotide-binding domain of Na^+, K^+-ATPase. Nat Struct Biol 10:468–4674
17. Haltia T, Freire E (1995) Forces and factors that contribute to the structural stability of membrane proteins. Biochim Biophys Acta 1241:295–322
18. Sampedro JG, Guerra G, Pardo JP, Uribe S (1998) Trehalose-mediated protection of the plasma membrane H^+-ATPase from *Kluyveromyces lactis* during freeze-drying and rehydration. Cryobiology 37:131–138
19. Ferreira ST (1993) Fluorescence lifetime and quenching studies of sarcoplasmic reticulum Ca(2+)-adenosine-5′-triphosphatase. Photochem Photobiol 58:195–199
20. Laws WR, Contino PB (1992) Fluorescence quenching studies: analysis of nonlinear Stern-Volmer data. Methods Enzymol 210: 448–463
21. Lacapere JJ, Bennett N, Dupont Y, Guillain F (1990) pH and magnesium dependence of ATP binding to sarcoplasmic reticulum ATPase. Evidence that the catalytic ATP-binding site consists of two domains. J Biol Chem 265:348–353
22. Dupont Y, Leigh JB (1978) Transient kinetics of sarcoplasmic reticulum Ca^{2+} /Mg^{2+} ATPase studied by fluorescence. Nature 273:396–398
23. Pratap PR, Mikhaylyants LO, Olden-Stahl N (2009) Fluorescence measurements of nucleotide association with the Na(+)/K(+)-ATPase. Biochim Biophys Acta 1794:1549–1557
24. Watanabe T, Inesi G (1982) The use of 2′,3′-O-(2,4,6-trinitrophenyl) adenosine 5′-triphosphate for studies of nucleotide interaction with sarcoplasmic reticulum vesicle. J Biol Chem 257:11510–11516
25. Fonseca MM, Scofano HM, Carvahlo-Alves PC, Barrabin H, Mignaco JA (2002) Conformational changes of the nucleotide site of the plasma membrane Ca^{2+}-ATPase probed by fluorescence quenching. Biochemistry 41:7483–7489
26. Vanderkooi JM, Ierokomas A, Nakamura H, Martonosi A (1976) Fluorescence energy transfer between Ca^{2+} transport ATPase molecules in artificial membranes. Biochemistry 16:1262–1267
27. Morgan CT, Tsivkovskii R, Kosinsky YA, Efremov RG, Lutsenko S (2004) The distinct functional properties of the nucleotide-binding domain of ATP7B, the human copper-transporting ATPase: analysis of the Wilson disease mutations E1064A, H1069Q, R1151H, and C1104F. J Biol Chem 279:36363–36371
28. Toyoshima C, Inesi G (2004) Structural basis of ion pumping by Ca^{2+}-ATPase of the sarcoplasmic reticulum. Annu Rev Biochem 73: 269–292
29. McIntosh DB, Clausen JD, Woolley DG, MacLennan DH, Vilsen B, Andersen JP (2006) ATP binding residues of sarcoplasmic reticulum Ca^{2+}-ATPase. Ann N Y Acad Sci 986:101–105
30. Abu-Abed M, Millet O, MacLennan DH, Ikura M (2004) Probing nucleotide-binding effects on backbone dynamics and folding of the nucleotide-binding domain of the sarcoplasmic/endoplasmic-reticulum Ca^{2+}-ATPase. Biochem J 379:235–242
31. Nakamura S, Susuki H, Kanazawa T (1994) The ATP-induced change of tryptophan fluorescence reflects a conformational change upon formation of ADP-sensitive phosphoenzyme in the sarcoplasmic reticulum Ca(2+)-ATPase. Stopped-flow spectrofluorometry and continuous flow-rapid quenching method. J Biol Chem 269:16015–16019
32. Myint W, Gong Q, Ahn J, Ishima R (2011) Characterization of sarcoplasmic reticulum Ca^{2+} ATPase nucleotide binding domain mutants using NMR spectroscopy. Biochem Biophys Res Commun 405:19–23
33. Kaler SG (2011) ATP7A-related copper transport diseases-emerging concepts and future trends. Nat Rev Neurol 7:15–29
34. Dmitriev OY, Bhattacharjee A, Nokhrin S, Uhleman E-ME, Lutsenko S (2011) Difference in stability of the N-domain underlies distinct intracellular properties of the E1064A and H1069Q mutants of copper-transporting ATPase ATP7B. J Biol Chem 286:16355–16362